$G_s\alpha$ enhances commitment of mesenchymal progenitors to the osteoblast lineage but restrains osteoblast differentiation in mice

Joy Y. Wu,[1] Piia Aarnisalo,[1,2,3] Murat Bastepe,[1] Partha Sinha,[1] Keertik Fulzele,[1] Martin K. Selig,[4] Min Chen,[5] Ingrid J. Poulton,[6] Louise E. Purton,[6] Natalie A. Sims,[6] Lee S. Weinstein,[5] and Henry M. Kronenberg[1]

[1]Endocrine Unit, Massachusetts General Hospital, Boston, Massachusetts, USA. [2]Institute of Biomedicine/Physiology, Biomedicum Helsinki, University of Helsinki, Finland. [3]Department of Clinical Chemistry, University of Helsinki and Helsinki University Central Hospital, Helsinki, Finland. [4]Department of Pathology, Massachusetts General Hospital, Boston, Massachusetts, USA. [5]Metabolic Diseases Branch, National Institute of Diabetes and Digestive and Kidney Diseases, Bethesda, Maryland, USA. [6]St. Vincent's Institute and Department of Medicine at St. Vincent's Hospital, The University of Melbourne, Fitzroy, Victoria, Australia.

The heterotrimeric G protein subunit $G_s\alpha$ stimulates cAMP-dependent signaling downstream of G protein–coupled receptors. In this study, we set out to determine the role of $G_s\alpha$ signaling in cells of the early osteoblast lineage in vivo by conditionally deleting $G_s\alpha$ from osterix-expressing cells. This led to severe osteoporosis with fractures at birth, a phenotype that was found to be the consequence of impaired bone formation rather than increased resorption. Osteoblast number was markedly decreased and osteogenic differentiation was accelerated, resulting in the formation of woven bone. Rapid differentiation of mature osteoblasts into matrix-embedded osteocytes likely contributed to depletion of the osteoblast pool. In addition, the number of committed osteoblast progenitors was diminished in both bone marrow stromal cells (BMSCs) and calvarial cells of mutant mice. In the absence of $G_s\alpha$, expression of sclerostin and dickkopf1 (Dkk1), inhibitors of canonical Wnt signaling, was markedly increased; this was accompanied by reduced Wnt signaling in the osteoblast lineage. In summary, we have shown that $G_s\alpha$ regulates bone formation by at least two distinct mechanisms: facilitating the commitment of mesenchymal progenitors to the osteoblast lineage in association with enhanced Wnt signaling; and restraining the differentiation of committed osteoblasts to enable production of bone of optimal mass, quality, and strength.

Introduction

Osteoporosis is one of the most common degenerative diseases of aging, with an estimated 50% of women experiencing an osteoporotic fracture during their lives. This skeletal fragility results from an imbalance between bone resorption and bone formation that is progressively exacerbated with age. At present the treatment of osteoporosis is largely dependent on antiresorptive agents, which increase bone density modestly and significantly reduce fracture risk, but cannot cure this degenerative disease (1). The ability to enhance the differentiation and function of osteoblasts would therefore be expected to have a profound impact on the treatment of osteoporosis. Indeed, recombinant parathyroid hormone (PTH) (teriparatide), the sole anabolic agent currently approved for clinical use in osteoporosis, is a potent stimulator of bone formation (2).

The actions of PTH on bone mass are complex and still incompletely understood. PTH is a ligand for the PTH/PTH-related peptide (PTHrP) receptor (PPR), a GPCR that activates multiple G protein–dependent signaling pathways (3). Signaling by the PPR has a significant effect on skeletal development, as targeted expression of the constitutively active mutant receptor to osteoblasts leads to a dramatic increase in the formation of trabecular bone (4). Activating mutations of the PPR, as found in Jansen metaphyseal chondrodysplasia, predominantly signal via the stimulatory G protein subunit $G_s\alpha$ in vitro (5). $G_s\alpha$ stimulates adenylyl cyclase and increases cAMP levels, resulting in activation of the PKA pathway (6). In humans, somatic activating mutations of $G_s\alpha$ are associated with fibrous dysplasia, expansile osteolytic lesions in which hematopoietic marrow is replaced by stromal cells of the osteoblast lineage, a phenotype reminiscent of the expansion of stromal cells seen in Jansen transgenic mice (7). When cells from fibrous dysplasia lesions are implanted subcutaneously, these cells, unlike normal cells from these patients, fail to differentiate into mature osteoblasts (8). Constitutive basal activation of $G_s\alpha$ by a modified GPCR has also been demonstrated to markedly increase the amount of trabecular bone in mice (9). These studies indicate that stimulation of $G_s\alpha$-dependent signaling in osteoblasts can profoundly affect bone mass.

However, the mechanisms by which $G_s\alpha$-dependent signaling regulates osteoblast differentiation remain obscure. Intermittent PTH increases osteoblast survival and differentiation (10). In contrast, continuous exposure to PTH in vitro significantly attenuates osteogenic differentiation, suggesting that under some circumstances PTH/PKA may inhibit osteoblast maturation (11, 12). In chondrocytes, ablation of either PPR or $G_s\alpha$ leads to accelerated chondrocyte differentiation and hypertrophy (13–17), demonstrating that PKA-dependent pathways can inhibit cellular differentiation in some tissues.

The canonical Wnt signaling pathway is required for the commitment and differentiation of mesenchymal progenitors to the osteoblast lineage. Ablation of β-catenin, a central component of canonical Wnt signaling, in early mesenchymal progenitors or osteoblast precursors leads to a failure of osteoblast commitment and differentiation, with adoption of a chondrocytic fate instead

Conflict of interest: The authors have declared that no conflict of interest exists.
Citation for this article: *J Clin Invest* doi:10.1172/JCI46406.

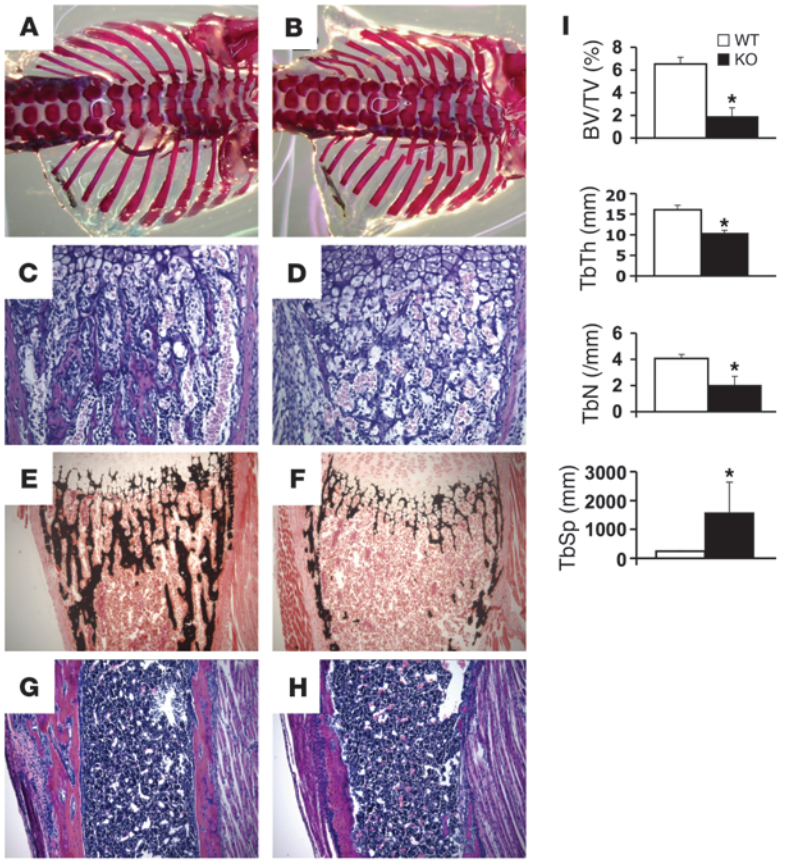

Figure 1
Deletion of $G_s\alpha$ in the osteoblast lineage leads to severe osteoporosis. (**A** and **B**) Skeletal preparations of mice at P1 in WT (**A**) and $G_s\alpha^{OsxKO}$ (KO) mice (**B**). (**C** and **D**) H&E-stained sections of primary spongiosa from WT (**C**) and KO (**D**) tibiae at E18.5. (**E** and **F**) Von Kossa staining of WT (**E**) and KO (**F**) proximal tibiae at 1 week. (**G** and **H**) H&E-stained sections of WT (**G**) and KO (**H**) mid-diaphyseal tibiae at 2 weeks. (**I**) Bone volume over trabecular volume (BV/TV), trabecular thickness (TbTh), trabecular number (TbN), and trabecular spacing (TbSp) in WT (white) and KO (black) mice at 1 week. $^*P < 0.01$ ($n = 7$ [WT] and $n = 5$ [KO]). Original magnification, ×200 (**C** and **D**), ×100 (**E**–**H**).

(18–20). In the skeleton, the PTH signaling pathway intersects with canonical Wnt signaling. For instance, PTH regulates several inhibitors of Wnt signaling (21). PTH suppresses expression of sclerostin, a canonical Wnt inhibitor encoded by *Sost* and produced by osteocytes, in a PKA-dependent manner (22, 23). MEF2 transcription factors acting on the Sost bone enhancer mediate this action of PTH (24). PTH also regulates dickkopf1 (Dkk1), another soluble Wnt inhibitor that blocks activation of the Wnt coreceptors Lrp5/6 (25). Although suppression of Dkk1 is not required for the anabolic effects of PTH (25, 26), overexpression of either Sost or Dkk1 results in osteopenia (27, 28). Conversely, targeted expression of a constitutively active PPR to osteocytes suppresses sclerostin expression and leads to high bone mass (29).

In addition to the PPR, several other GPCRs that signal via $G_s\alpha$ have been described in osteoblasts, including receptors for PGE_2 (EP2R and EP4R) (30), thyroid-stimulating hormone (31), and β_2-adrenergic agonists (32). Ablation of these receptors leads to varying and sometimes opposing skeletal consequences in mice. Since $G_s\alpha$ likely serves to mediate signaling downstream of multiple GPCRs in osteoblasts, we hypothesized that ablation of $G_s\alpha$ early in the osteoblast lineage would have significant effects on osteoblast differentiation. Ablation of $G_s\alpha$ in more differentiated cells of the osteoblast lineage results in reduced trabecular bone and increased cortical bone late in embryogenesis (33). However, craniofacial abnormalities and perinatal lethality have precluded the analysis of the role of $G_s\alpha$ in early postnatal development of the skeleton.

In an article describing the regulation of B lymphocyte development in the bone marrow by cells of the osteoblast lineage, we have previously reported that ablation of $G_s\alpha$ early in the osteoblast lineage results in postnatal growth retardation and early mortality, with a dramatic decrease in the bone surface covered with trabecular osteoblasts (34). We now demonstrate that absence of $G_s\alpha$ dramatically impairs bone formation, and we identify at least two distinct functions for $G_s\alpha$ in cells of the osteoblast lineage. First, differentiation of $G_s\alpha$-deficient osteoblasts is significantly accelerated, resulting in the formation of predominantly woven bone that is highly susceptible to fractures. Second, in the absence of $G_s\alpha$, expression of the Wnt inhibitors sclerostin and Dkk1 is significantly upregulated, with attenuation of Wnt signaling in osteoblasts. Consistent with previous reports that the commitment of mesenchymal progenitors to the osteoblast lineage is dependent upon canonical Wnt signaling (18–20), we found that the frequency of osteoblast precursors is markedly decreased in mutant mice.

Results

Deletion of $G_s\alpha$ in osteoprogenitors leads to profound osteoporosis. Mice lacking $G_s\alpha$ in the osteoblast lineage ($G_s\alpha^{OsxKO}$ mice) were generated by ablation of $G_s\alpha$ in osterix-expressing (Osx-expressing) progenitors as previously described (34). Mutant mice were grossly similar to control littermates at birth, and skeletal preparations did not demonstrate significant differences in patterning of the axial skeleton on P1 (Supplemental Figure 1, A and B; supplemental material available online with this article; doi:10.1172/JCI46406DS1). Histological analysis at E15.5 revealed normal vascular invasion, with subsequent formation of the bone marrow cavity (Supplemental Figure 1, C and D). However, fractures

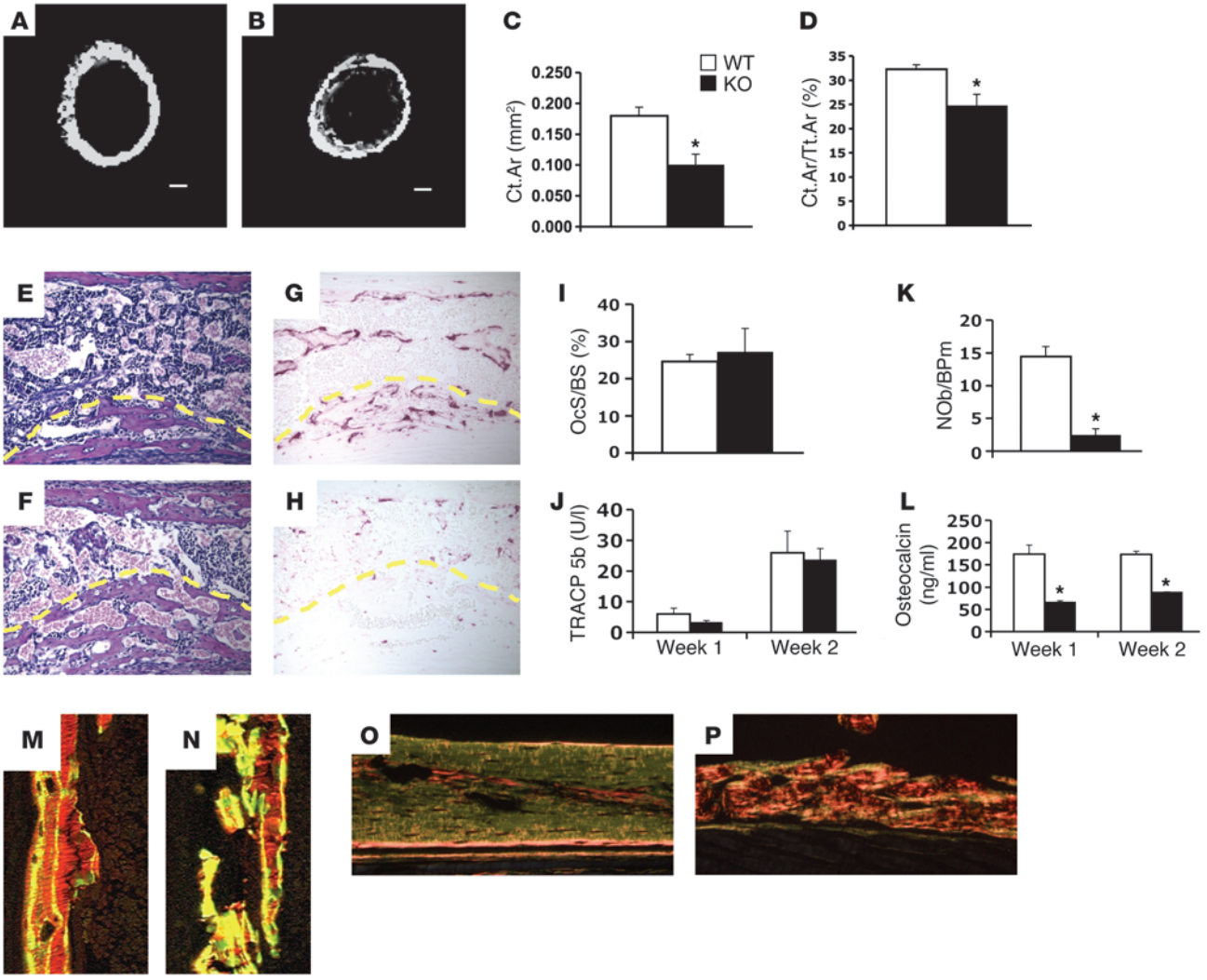

Figure 2

Decreased bone mass in the absence of $G_s\alpha$ is due to inadequate bone formation. (**A**–**D**) Micro-CT of WT (**A**) and KO (**B**) femurs at 1 week. Cortical bone area (Ct.Ar) (**C**) and cortical area fraction (Ct.Ar/Tt.Ar) (**D**) at 1 week. *$P < 0.05$ ($n = 5$ [WT] and $n = 3$ [KO]). (**E**–**H**) H&E- (**E** and **F**) and TRAP-stained (**G** and **H**) sections of cortical bone from WT (**E** and **G**) and KO (**F** and **H**) tibiae at E18.5. Dashed yellow line denotes the endocortical edge of cortical bone. (**I**) Osteoclast surface per bone surface (OcS/BS, $n = 7$ [WT] and $n = 5$ [KO]). (**J**) Serum TRACP 5b levels ($n = 6$ per genotype). (**K**) Osteoblast number per bone perimeter (NOb/BPm). *$P < 0.001$ ($n = 7$ [WT] and $n = 5$ [KO]). (**L**) Serum osteocalcin levels. *$P < 0.01$ ($n = 6$ per genotype). (**M** and **N**) Double calcein labeling in WT (**M**) and KO (**N**) cortical bone at week 1. (**O** and **P**) Cortical bone from WT (**O**) and KO (**P**) mice at 2 weeks stained with Sirius red and photographed under polarized light. Scale bars: 100 μm (**A** and **B**). Original magnification, ×200 (**E**–**H**, **M**, and **N**), ×400 (**O** and **P**).

of ribs (Figure 1, A and B) and long bones (Supplemental Figure 1, E and F) were identified in $G_s\alpha^{OsxKO}$ mice on P1. Perhaps as a consequence of early and extensive fractures, although other contributing factors have not been ruled out, $G_s\alpha^{OsxKO}$ mice exhibit early postnatal mortality (ref. 34 and Supplemental Figure 1G), with no mutant mice surviving until weaning. The fractures did not occur simply as a result of handling of the skeletons during isolation, as healing calluses were evident by 1 week of life (Supplemental Figure 1, H and I). The fractures were not present in utero (Supplemental Figure 1, J–L), suggesting that initial fractures were sustained during birth. However, delivery via Caesarian section failed to prevent early postnatal acquisition of fractures and did not reduce mortality (data not shown).

Sakamoto et al. reported that ablation of $G_s\alpha$ in differentiated osteoblasts using collagen Iα1 promoter Cre transgenic mice resulted in reduced trabecular bone at E18.5 (33). We found that deletion of $G_s\alpha$ earlier in the osteoblast lineage also led to reduced trabecular bone in the primary spongiosa at E18.5 (Figure 1, C and D). By 1 week of age, von Kossa staining demonstrated further loss of mineralized trabecular bone (Figure 1, E and F). Cortical bone was markedly irregular and thinned in the few mice surviving past the second week of life, and in places was almost completely absent (Figure 1, G and H). Histomorphometric analysis of the tibial metaphysis revealed a 71% decrease in trabecular bone volume, with decreased trabecular thickness and number and increased trabecular spacing (Figure 1I).

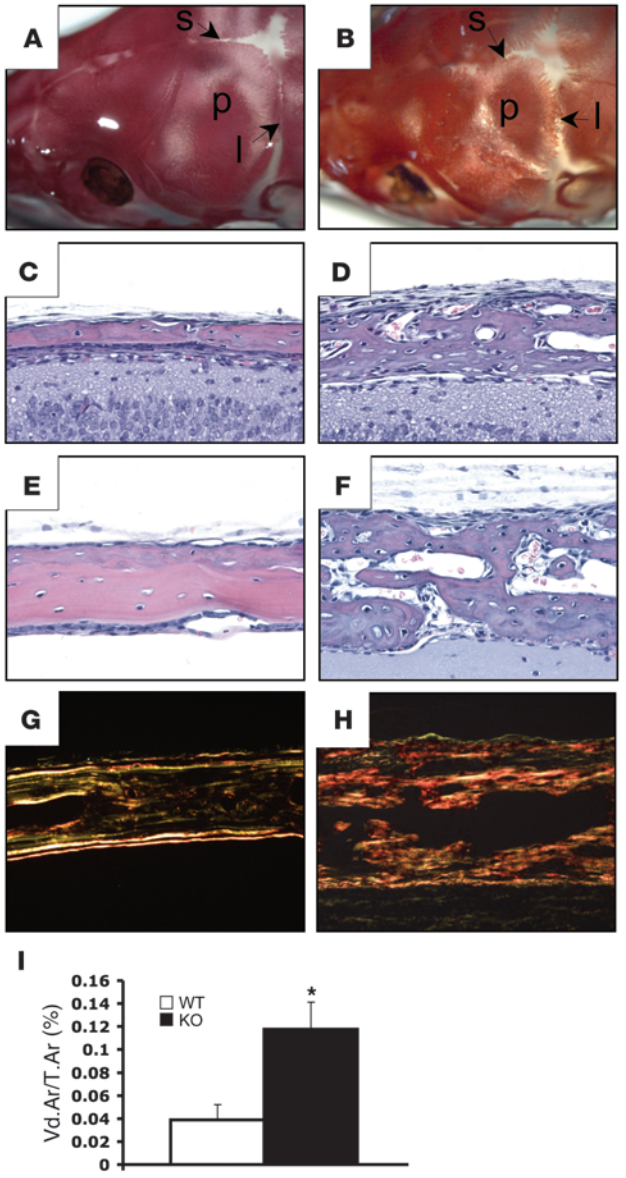

Figure 3
Intramembranous bone formation is defective in $G_s\alpha^{OsxKO}$ mice. (**A** and **B**) Skeletal preparations of calvariae of WT (**A**) and KO (**B**) mice at P1. p, parietal bone; s, sagittal suture; l, lambdoid suture. (**C**–**F**) H&E-stained calvarial sections at P4 (**C** and **D**) and 2 weeks (**E** and **F**) in WT (**C** and **E**) and KO (**D** and **F**) mice. (**G** and **H**) Sirius red–stained sections of WT (**G**) and KO (**H**) calvarial bone at 2 weeks photographed under polarized light. (**I**) Cortical porosity void area (VD.Ar/T.Ar) in WT and KO mice at 2 weeks of age. $^*P < 0.05$ ($n = 4$ per genotype). Original magnification, ×400 (**C**–**H**).

Decreased bone mass in the absence of $G_s\alpha$ is due to impaired bone formation rather than enhanced bone resorption. Micro-CT demonstrated reduced cortical bone and increased cortical porosity at 1 week (Figure 2, A–D). To determine whether the porosity might result from enhanced bone resorption by osteoclasts, we performed TRAP staining at E18.5, when cortical bone had not yet thinned significantly in $G_s\alpha^{OsxKO}$ mice (Figure 2, E and F). As previously reported for ablation of $G_s\alpha$ in differentiated osteoblasts (33), there was a marked decrease in the number of endocortical osteoclasts at E18.5 (Figure 2, G and H). Furthermore, at no time during early postnatal development was there evidence for increased numbers of $TRAP^+$ osteoclasts in trabecular bone of mutant mice (data not shown). Osteoclast surface was not increased in trabecular bone of 1-week-old mutant mice (Figure 2I), and there was no increase in the level of serum TRACP 5b, a marker of bone resorption, despite the presence of fractures (Figure 2J). These findings suggest that the dramatic decrease in $G_s\alpha^{OsxKO}$ bone mass cannot be attributed to increased bone resorption.

If the decreased bone mass in $G_s\alpha^{OsxKO}$ mice was not the result of enhanced bone resorption, then bone formation must have been inadequate. Consistent with this, histomorphometry revealed an 85% reduction in osteoblast surface (34) and an equally dramatic decrease in osteoblast number in $G_s\alpha^{OsxKO}$ mice (Figure 2K). Serum osteocalcin, a marker of bone formation, was also significantly decreased in early postnatal mutant mice (Figure 2L). In an attempt to calculate bone formation rate by dynamic histomorphometry, we performed double calcein labeling 1 and 4 days prior to analysis on P7. In control mice this allowed visualization of two distinct mineralization fronts (Figure 2M). In contrast, bones from mutant mice were diffusely labeled with fluorochrome, indicating the formation of woven bone during the labeling period and precluding analysis of bone formation rate (Figure 2N). Indeed, when tibiae of 2-week-old mice were analyzed under polarized light, the cortical bone of control mice exhibited lamellar organization, while mutant cortical bone revealed markedly disorganized arrangement of collagen fibrils (Figure 2, O and P). Together these results indicate that the loss of $G_s\alpha$ early in the osteoblast lineage leads to formation of disorganized bone of insufficient mass, strength, and quality, as evidenced by the occurrence of fractures.

Intramembranous bone formation is defective in $G_s\alpha^{OsxKO}$ mice. While long bones are formed by the process of endochondral ossification, craniofacial bones are more commonly derived by intramembranous ossification, in which cells of mesenchymal condensations differentiate directly into osteoblasts without a cartilage template. Skeletal preparations on P1 demonstrated a dramatic impairment in mineralization of intramembranous cranial bones. While the parietal bone of control mice exhibited relatively homogenous mineralization and well-formed sutures (Figure 3A), the parietal bone in $G_s\alpha^{OsxKO}$ mice displayed patchy mineralization in a reticular pattern with ragged sutures (Figure 3B). Histological analysis of control calvariae at P4 and 2 weeks revealed 1–2 layers of osteoblasts along the bone surfaces and orderly lamellar bone (Figure 3, C and E). In contrast, multiple layers of stromal cells and preosteoblasts were found lining the periosteal surface of $G_s\alpha^{OsxKO}$ mice (Figure 3, D and F). Like cortical bone, the calvarial bone of $G_s\alpha^{OsxKO}$ mice was woven, as indicated by misshapen osteocyte lacunae and irregular collagen fibril deposition (Figure 3, G and H). Likewise, porosity was dramatically increased in $G_s\alpha^{OsxKO}$ calvarial bones at 2 weeks (Figure 3I). Therefore ablation of $G_s\alpha$ early in the osteoblast lineage resulted in abnormal trabecular, cortical, and intramembranous bone that was evident at birth, indicating that $G_s\alpha$ plays a crucial role during embryonic skeletogenesis.

Osteogenic differentiation is accelerated in the absence of $G_s\alpha$. To assess osteoblast differentiation in vivo in the absence of $G_s\alpha$, we analyzed the expression of gene markers of osteoblast differentiation. We found that during embryonic development, mRNA levels of genes expressed early in the osteoblast lineage, such as alkaline phosphatase

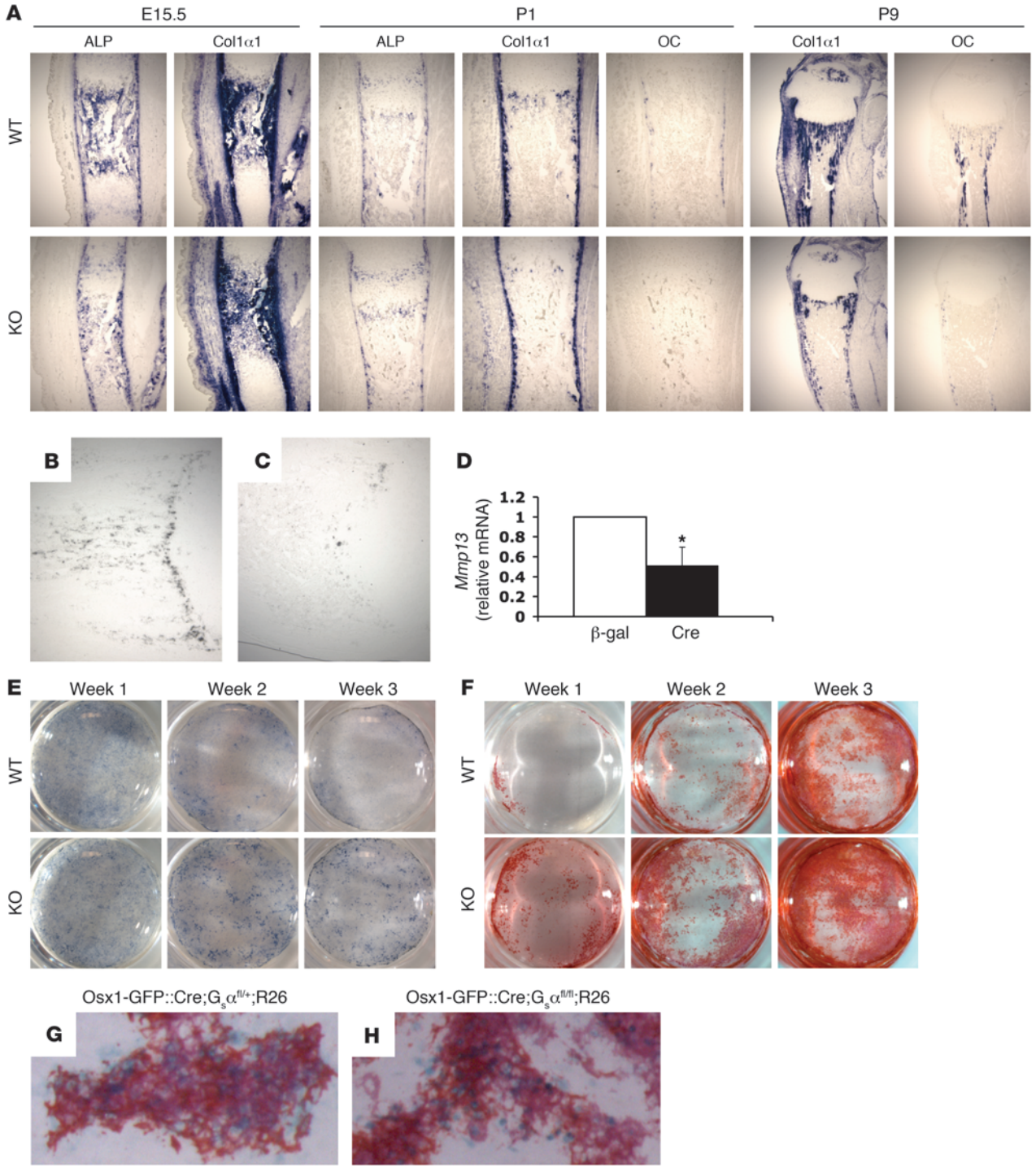

Figure 4

Osteogenic differentiation is not impaired in $G_s\alpha^{OsxKO}$ mice. (**A**) In situ hybridization for osteogenic markers ALP, collagen Iα1 (Col1α1), and osteocalcin (OC). (**B** and **C**) In situ hybridization for MMP-13 expression in WT (**B**) and KO (**C**) proximal tibiae at P7. (**D**) *Mmp13* mRNA levels in $G_s\alpha^{fl/fl}$ calvarial osteoblasts infected with control adenovirus (β-gal) or Cre recombinase. $^*P < 0.05$ ($n = 5$). (**E**) ALP staining and (**F**) alizarin staining of calvarial osteoblast cells undergoing osteogenic differentiation. Results are representative of 5 experiments. (**G** and **H**) Calvarial osteoblasts were harvested from control or KO mice crossed to R26 reporter mice, then subjected to osteogenic differentiation. After 21 days in culture, wells were stained with alizarin to highlight mineral deposition and X-gal to identify cells descended from Osx^+ precursors in control (**G**) and KO (**H**) mice. Original magnification, ×100 (**A**, E15.5 and P1), ×40 (**A**, P9), ×400 (**G** and **H**).

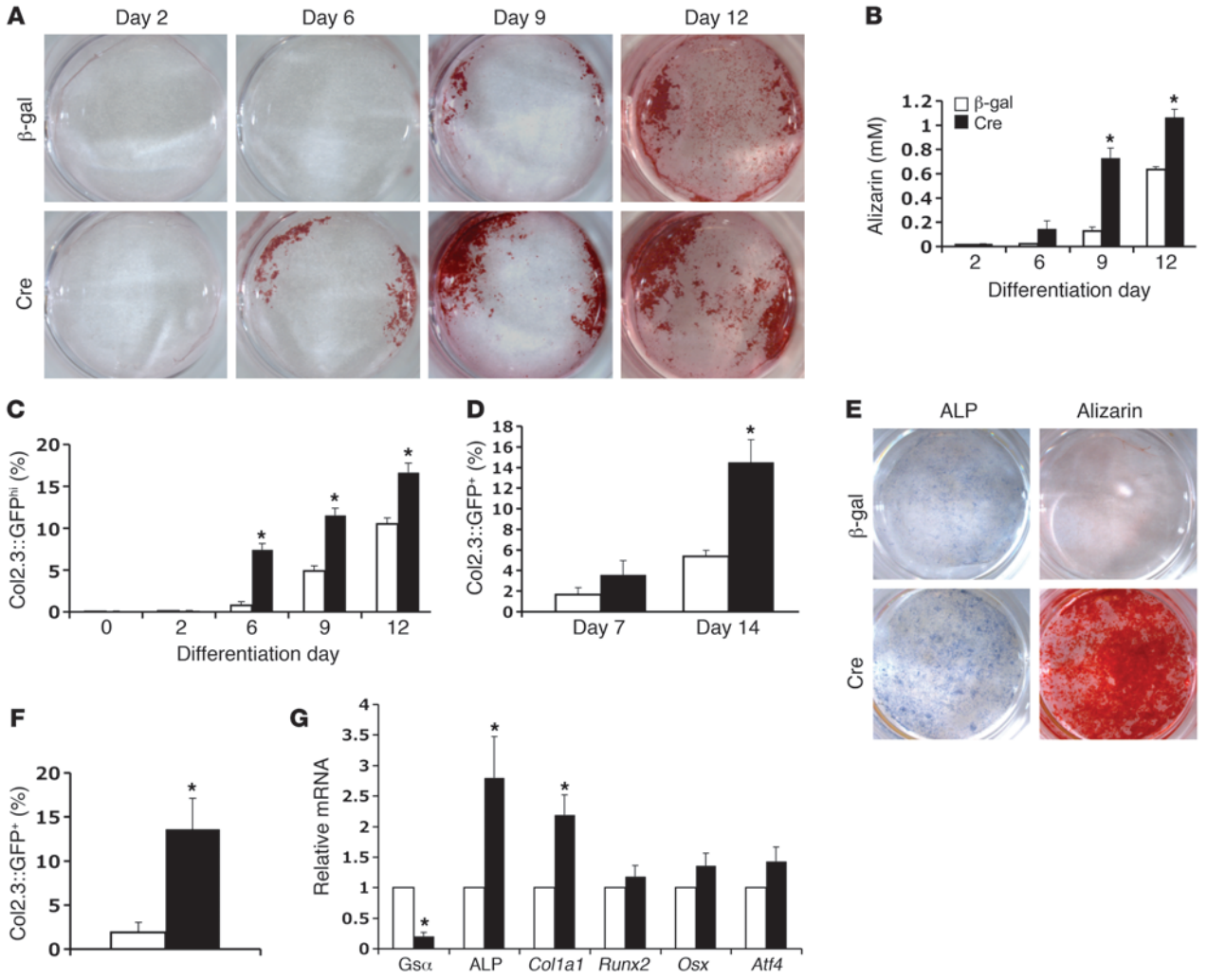

Figure 5

Osteogenic differentiation is accelerated in the absence of $G_s\alpha$. (**A**–**C**) Alizarin staining (**A** and **B**) and frequency of Col2.3::GFP^{hi} cells in Col2.3::GFP;$G_s\alpha^{fl/fl}$ calvarial cells infected with adeno-Cre or adeno–β-gal and subjected to osteogenic differentiation (**C**). *$P < 0.05$ ($n = 3$). (**D**) Frequency of Col2.3::GFP$^+$ cells in sorted ALP$^-$ cells from Col2.3::GFP;$G_s\alpha^{fl/fl}$ mice subjected to osteogenic differentiation. *$P < 0.05$ ($n = 4$). (**E**) $G_s\alpha^{fl/fl}$ BMSCs infected with adeno-β-gal or adeno-Cre and induced to undergo osteogenic differentiation, then stained with ALP or alizarin after 2 weeks in culture. (**F**) Frequency of Col2.3::GFP$^+$ cells in BMSCs from Col2.3::GFP;$G_s\alpha^{fl/fl}$ mice after 2 weeks of osteogenic differentiation. *$P < 0.02$ ($n = 3$). (**G**) mRNA levels for $G_s\alpha$, ALP, collagen Iα1 (*Col1a1*), *Runx2*, *Osx*, and *Atf4* in $G_s\alpha^{fl/fl}$ calvarial osteoblasts infected with adeno-Cre or adeno–β-gal and induced to undergo osteogenic differentiation for 6 days. *$P < 0.05$ ($n = 3$–5 experiments).

(ALP) and collagen Iα1, were similar in $G_s\alpha^{OsxKO}$ mice and littermate controls at E15.5 and P1 (Figure 4A). In contrast, expression of osteocalcin mRNA, a marker of terminally differentiated osteoblasts initially detectable in WT mice at P1, was nearly absent in mutant bones by P9 (Figure 4A). By this time collagen Iα1 expression was also noticeably decreased, likely reflecting the dramatic decrease in osteoblast numbers (Figure 2K). Since osteocalcin mRNA expression is at least partly dependent on PKA-mediated gene transcription (35), its absence could reflect reduced PKA activation in osteoblasts lacking $G_s\alpha$. Consistent with this, expression of another PKA target gene, *Mmp13* (36), was also reduced in bones from $G_s\alpha^{OsxKO}$ mice (Figure 4, B and C) as well as $G_s\alpha$-deficient osteoblasts (Figure 4D). However, given the markedly reduced osteoblast number in mutant mice, the absence of osteocalcin expression might also reflect failure of terminal differentiation into mature osteoblasts in the absence of $G_s\alpha$.

In order to evaluate osteoblast differentiation directly, we isolated primary calvarial osteoblastic cells from $G_s\alpha^{OsxKO}$ mice and control littermates, and subjected these cells to osteogenic differentiation in vitro. Unexpectedly, $G_s\alpha^{OsxKO}$ cells consistently demonstrated accelerated ALP expression as well as earlier and more extensive mineralization than cells from WT mice (Figure 4, E and F). To demonstrate that the accelerated differentiation occurred in cells in which Cre recombinase had been active, we crossed $G_s\alpha^{OsxKO}$ mice to R26 reporter mice (37). In Osx1-GFP::Cre;$G_s\alpha^{fl/fl}$;R26 mice, cells stained blue by X-gal reflect expression of Cre recombinase and therefore likely ablation of $G_s\alpha$. We have previously shown that expression of Cre recombinase efficiently reduces $G_s\alpha$ mRNA levels by greater than 90% (34). We found that calvarial osteoblasts from Osx1-GFP::Cre;$G_s\alpha^{fl/fl}$;R26 mice, as well as control Osx1-GFP::Cre;$G_s\alpha^{fl/+}$;R26 mice, formed mineralized

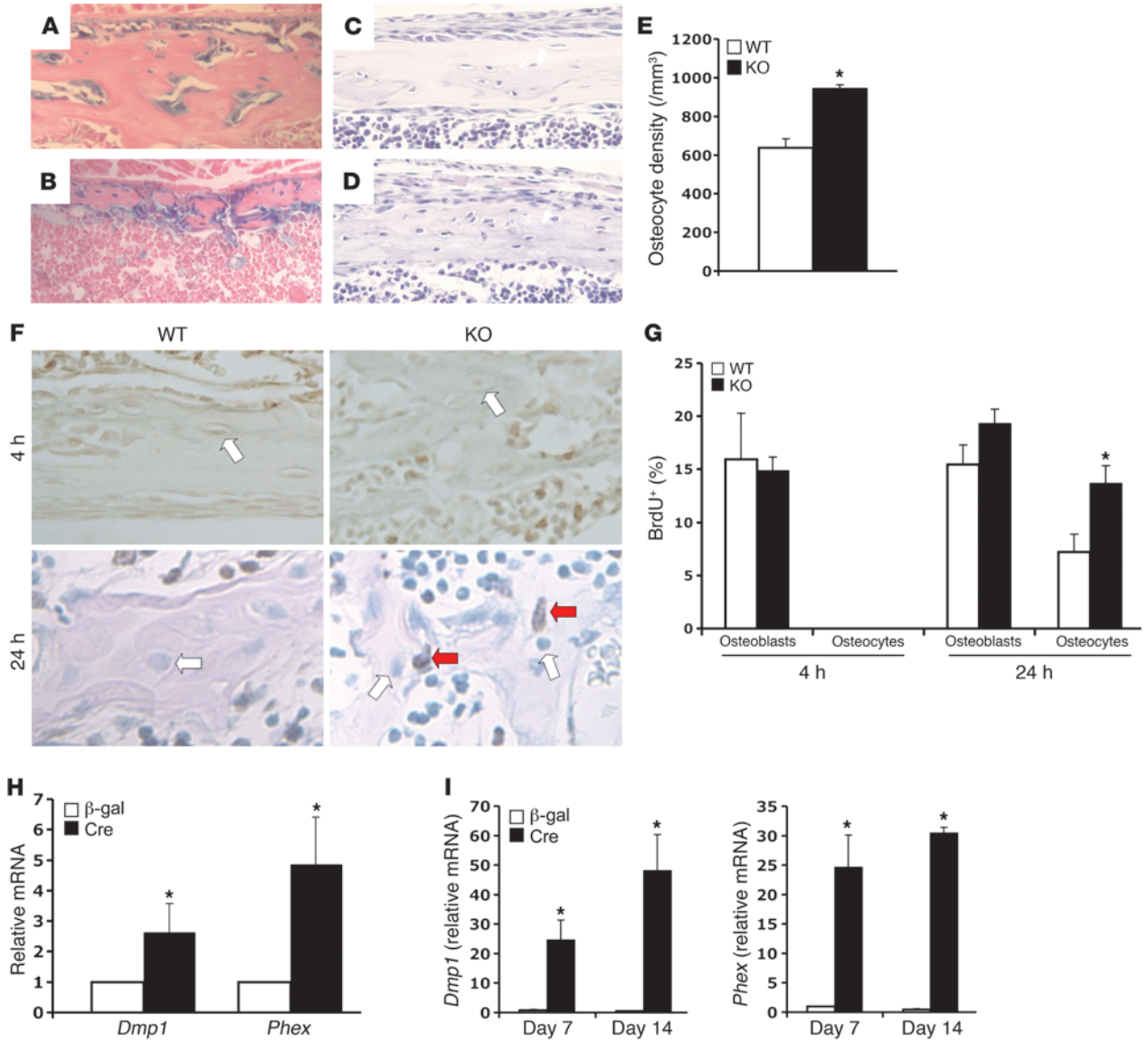

Figure 6

Accelerated osteogenic differentiation occurs in vivo in $G_s\alpha^{OsxKO}$ mice. (**A** and **B**) X-gal staining of cortical bone at P7 from WT (**A**) and KO (**B**) mice crossed to R26 reporter mice. (**C** and **D**) H&E-stained sections of cortical bone from tibiae of WT (**C**) and KO (**D**) mice at P7. (**E**) Osteocyte density in cortical bone of tibiae at P7. *$P < 0.005$ ($n = 3$). (**F**) BrdU pulse-chase in WT and KO trabecular bone of tibiae at P4. White arrows indicate BrdU-negative osteocytes; red arrows indicate BrdU-positive osteocytes. (**G**) Frequency of BrdU$^+$ osteocytes and osteoblasts 4 and 24 hours after injection. *$P < 0.05$ ($n = 3$). (**H** and **I**) mRNA levels of osteocyte markers *Dmp1* and *Phex* in $G_s\alpha^{fl/fl}$ calvarial osteoblasts (**H**) ($n = 6$) and bone marrow stromal cells (**I**) ($n = 3$) infected with adeno-Cre (black) or adeno–β-gal (white) and induced to undergo osteogenic differentiation for 1 (**H**) or 2 (**I**) weeks. *$P < 0.05$. Original magnification, ×400 (**A**–**D**), ×1,000 (**F**).

nodules in which the majority of cells in the nodule were also blue (Figure 4, G and H). Therefore, in calvarial osteoblasts isolated from $G_s\alpha^{OsxKO}$ mice and subjected to osteogenic differentiation, the enhanced mineralization was a direct effect of $G_s\alpha$ deficiency in cells of the osteoblast lineage.

Since calvariae from $G_s\alpha^{OsxKO}$ mutant mice exhibit impaired mineralization (Figure 3B), we considered the possibility that the results of Figure 4, E and F, might be explained by an artifact: perhaps serial collagenase digestion would more easily recover differentiated osteoblasts from mutant calvariae than from control calvariae, thereby favoring the onset of mineralization in cells isolated from mutant mice. To control for the distribution of osteoblast lineage populations at varying stages of differentiation, we harvested primary calvarial osteoblasts from Col2.3::GFP;$G_s\alpha^{fl/fl}$ mice, in which GFP is under the control of the 2.3-kb rat type I collagen promoter and therefore expressed in differentiated osteoblasts (38). In cells isolated from calvariae of these mice, expression of GFP serves as a marker for osteogenic differentiation (12, 38). Equal numbers of calvarial cells from Col2.3::GFP;$G_s\alpha^{fl/fl}$ mice were infected with either adenovirus encoding Cre recombinase to ablate $G_s\alpha$ expression or

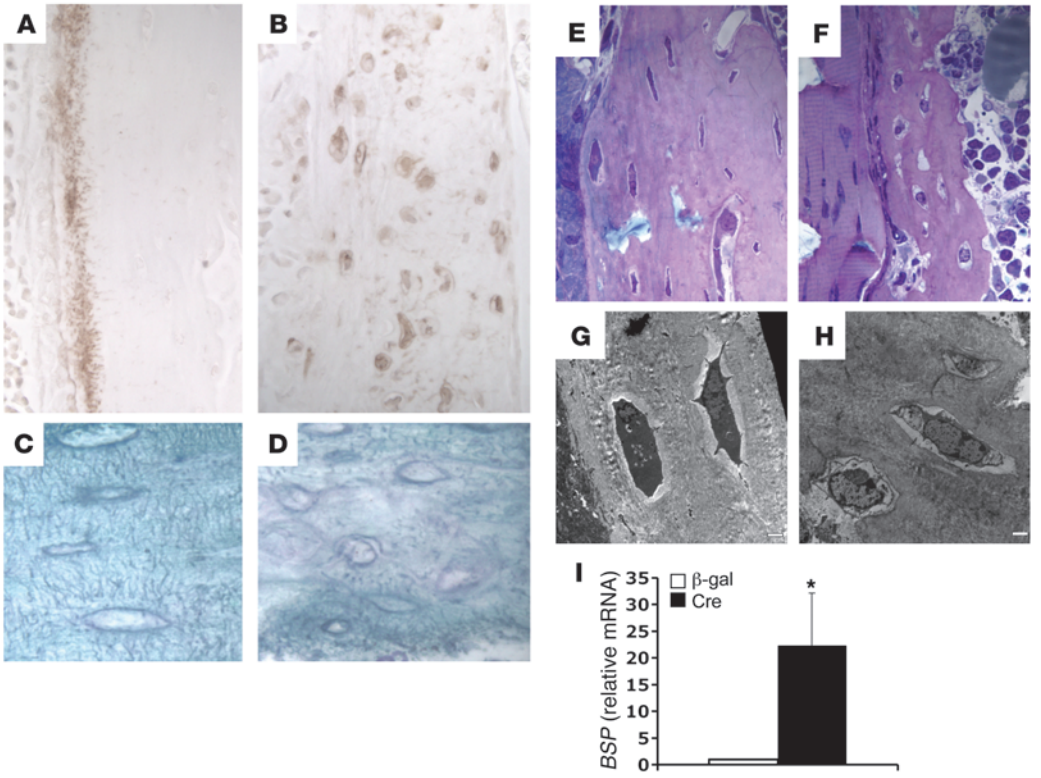

Figure 7
Accelerated osteoblast maturation in $G_s\alpha^{OsxKO}$ mice is associated with woven bone and abnormal osteocytes. (**A** and **B**) Anti-E11 immunohistochemical staining in cortical bone of WT (**A**) and KO (**B**) tibiae at week 3. (**C** and **D**) Bodian staining of the osteocyte lacuno-canalicular network in WT (**C**) and KO (**D**) mice at week 3. (**E** and **F**) Toluidine blue staining of osteocytes in WT (**E**) and KO (**F**) cortical bone at week 2. (**G** and **H**) Transmission electron microscopy of WT (**G**) and KO (**H**) osteocytes. (**I**) mRNA level of *BSP* in differentiating $G_s\alpha^{fl/fl}$ calvarial osteoblasts. $^*P < 0.05$ ($n = 7$). Original magnification, ×400 (**A**, **B**, **E**, and **F**), ×1,000 (**C** and **D**), ×3,400 (**G** and **H**).

with control adenovirus encoding either β-gal or YFP. $G_s\alpha$ expression was efficiently reduced within 24 hours (Supplemental Figure 2A), and functional loss of $G_s\alpha$ was confirmed by the decrease in basal cAMP levels after 48 hours (Supplemental Figure 2B), after which cells were placed in osteogenic differentiation media. Cre-infected $G_s\alpha$-deficient cells displayed robust mineralization as early as 6 days after differentiation, while mineralization of control cells was not detectable until 9 days in culture (Figure 5, A and B). The Col2.3::GFP$^+$, and in particular the GFP^{hi}, population was enriched in cells that expressed markers of mature osteoblasts (ALP, collagen Iα1, and osteocalcin) (Supplemental Figure 2, C and D). GFP expression was significantly increased in Cre-infected cells by day 6 and remained persistently elevated relative to control cells throughout the course of differentiation (Figure 5C). Mineralization in vitro can be affected by cell density; however, we confirmed that the enhanced mineralization of Cre-infected $G_s\alpha$-deficient calvarial osteoblasts was independent of cell number. When plated at low cell density such that there was a moderate increase in cell number in $G_s\alpha$-deficient cells only after 12 days in culture (Supplemental Figure 2E), there was already a significant increase in both alizarin deposition (Supplemental Figure 2F) and the frequency of Col2.3::GFP^{hi} cells (Supplemental Figure 2G) after 6 days of culture. These differences were even more pronounced after 12 days in culture. To determine whether $G_s\alpha$ deletion accelerated the differentiation only of committed osteoprogenitors, we sorted ALP$^-$ Col2.3::GFP$^-$ $G_s\alpha^{fl/fl}$ cells, which do not yet express markers of osteogenic commitment (Supplemental Figure 2D), infected them with adeno-Cre or adeno–β-gal, and subjected them to osteogenic differentiation. Even among uncommitted progenitors, ablation of $G_s\alpha$ led to enhanced osteogenic differentiation (Figure 5D). Finally, the accelerated osteogenic differentiation in cells lacking $G_s\alpha$ was not unique to calvarial osteoblasts. Bone marrow stromal cells (BMSCs) isolated from Col2.3::GFP;$G_s\alpha^{fl/fl}$ mice and infected with adeno-Cre also demonstrated dramatic enhancement of osteogenic differentiation (Figure 5, E and F).

We next analyzed markers of osteoblast differentiation in cultured calvarial osteoblasts (Figure 5G). After 6 days of culture under osteogenic conditions, $G_s\alpha$ mRNA expression remained significantly reduced by adeno-Cre infection. Accelerated maturation was reflected by the significant increase in expression of the osteoblast markers ALP and collagen Iα1 in $G_s\alpha$-deficient cells relative to control cells. However, we did not detect any significant differences in the mRNA levels of the osteogenic transcription factors *Runx2*, *Osx*, or *Atf4*. Together these data demonstrate that osteogenic differentiation is dramatically accelerated when $G_s\alpha$ is deleted early in the osteoblast lineage.

Osteoblast differentiation is accelerated in vivo in $G_s\alpha^{OsxKO}$ mice. In order to assess the fate of $G_s\alpha$-deficient cells of the osteoblast lineage in vivo, we crossed $G_s\alpha^{OsxKO}$ to Rosa26 reporter mice (37). Staining with X-gal revealed abundant cells in $G_s\alpha^{OsxKO}$ bone that were descended

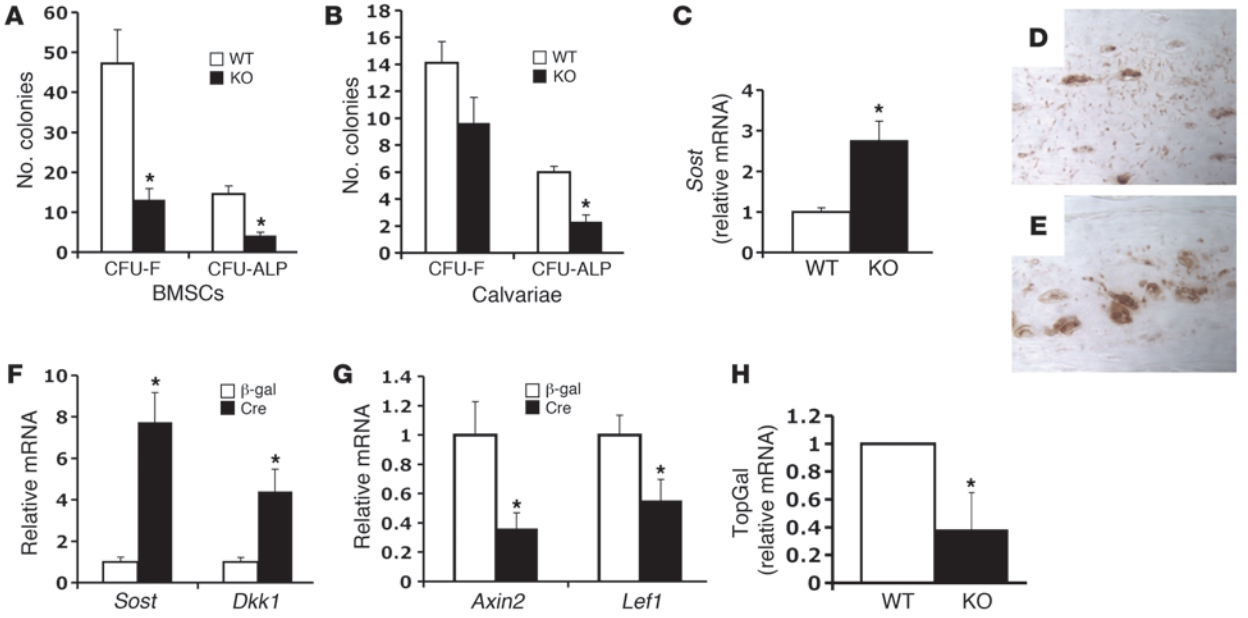

Figure 8

$G_s\alpha^{OsxKO}$ mice have reduced Wnt signaling in the osteoblast lineage and a depleted osteoprogenitor pool. (**A** and **B**) CFU-F and CFU-ALP assays in WT and KO BMSCs (**A**) and calvarial cells (**B**). *$P < 0.01$ ($n = 6–9$). (**C**) *Sost* mRNA levels in calvariae of WT and KO mice. *$P < 0.01$ ($n = 6$). (**D** and **E**) Immunohistochemical staining for sclerostin protein in WT (**D**) and KO (**E**) tibia at week 3. (**F**) mRNA levels of *Sost* and *Dkk1* and (**G**) Wnt target genes *Axin2* and *Lef1* in $G_s\alpha^{fl/fl}$ calvarial osteoblasts infected with adeno-Cre (black) or adeno–β-gal (white) and induced to undergo osteogenic differentiation. *$P < 0.05$ ($n = 3$). (**H**) TopGal mRNA levels in calvariae of WT and KO mice crossed to TopGal reporter mice. *$P < 0.05$ ($n = 3$). Original magnification, ×400 (**D** and **E**).

from Osx-expressing precursors, including osteocytes (Figure 6, A and B). Osteocytes are derived from terminally differentiated osteoblasts (39, 40) and are embedded in the mineralized matrix. Indeed, inspection of H&E-stained sections of both cortical and calvarial bones revealed a significant increase in osteocyte density in $G_s\alpha^{OsxKO}$ mice (Figure 6, C–E, and data not shown). To determine whether accelerated osteoblast maturation might contribute to the increased osteocyte density in $G_s\alpha^{OsxKO}$ mice, we performed a pulse-chase with BrdU. Four hours after BrdU injection, no $BrdU^+$ osteocytes were identified, consistent with their postmitotic state. In contrast, 24 hours after BrdU injection, we found a significantly higher proportion of $BrdU^+$ osteocytes in $G_s\alpha^{OsxKO}$ mice relative to littermate controls (Figure 6, F and G). Since osteocytes themselves do not proliferate and therefore do not incorporate BrdU, $BrdU^+$ osteocytes must have been derived from labeled pre-osteoblasts/osteoblasts that subsequently differentiated into osteocytes. We could find no discernible increase in $BrdU^+$ frequency in $G_s\alpha^{OsxKO}$ mature osteoblasts on the bone surface at either 4 or 24 hours after injection, suggesting that enhanced differentiation rather than increased proliferation of osteoblasts leads to the increased frequency of $BrdU^+$ osteocytes in $G_s\alpha^{OsxKO}$ mice (Figure 6, F and G). To further investigate osteoblast proliferation in vivo, we isolated Osx1-GFP::Cre^+ osteoblasts by FACS sorting from WT and $G_s\alpha^{OsxKO}$ mice. Cell cycle analysis demonstrated that the distribution of cells in cell cycle stages G_1, S, and G_2/M was the same in Osx1-GFP::Cre^+ cells from control (Osx1-GFP::Cre+;$G_s\alpha^{+/+}$) and $G_s\alpha^{OsxKO}$ mice, again indicating similar rates of proliferation of these cells in vivo (Supplemental Figure 3A). Finally, TUNEL staining for the presence of apoptosis did not reveal any significant increase in apoptosis of $G_s\alpha^{OsxKO}$ osteoblasts in tibiae at 1 week (Supplemental Figure 3, B and C).

In vitro, expression of osteocytic markers coincides with mineralized nodule formation (41). We therefore examined expression of osteocyte-specific genes in calvarial osteoblasts cultured under osteogenic conditions, and found that after only 1 week in culture, expression of the osteocyte-specific genes *Dmp1* and *Phex* was upregulated in mutant calvarial osteoblasts, coincident with the early appearance of mineralization (Figure 6H). Similarly, *Dmp1* and *Phex* mRNA levels were dramatically increased over 2 weeks of osteogenic differentiation of $G_s\alpha$-deficient BMSCs (Figure 6I). In summary, these data indicate that both in vitro and in vivo, absence of $G_s\alpha$ leads to accelerated osteoblast differentiation in a cell-autonomous manner. The rapid maturation of differentiated osteoblasts into osteocytes therefore contributes to the small size of the mature osteoblast pool in $G_s\alpha^{OsxKO}$ mice.

$G_s\alpha^{OsxKO}$ mice have woven bone and abnormal osteocytes. The osteocytes in $G_s\alpha^{OsxKO}$ mice that result from accelerated osteoblast differentiation display numerous abnormalities characteristic of woven bone. E11 is a marker of early osteocytes and/or late osteoblasts and plays a role in the elongation of osteocytic dendrites (42). In tibiae of control mice, expression of E11 protein in cortical bone was restricted to a single layer of cells, representing terminally differentiated osteoblasts and/or immature osteocytes, at the edge of the mineralizing matrix, highlighting the dendritic processes that form the osteocyte lacuno-canalicular network (Figure 7A). In contrast, expression of E11 in tibiae of mutant mice was found throughout the thickness of cortical bone in osteocytes with a notable paucity of dendrites (Figure 7B). We confirmed disruption of the normal osteocyte lacuno-canalicular network with Bodian staining, which revealed a well-established network in control mice but the absence of a well-organized canalicular net-

work in mutant bones (Figure 7, C and D). Furthermore, osteocyte morphology was abnormal in $G_s\alpha^{OsxKO}$ bones, with rounded nuclei and increased perilacunar space (Figure 7, E and F). Transmission electron microscopy further demonstrated that whereas control cells have abundant cytoplasm containing rough endoplasmic reticulum, mutant osteocytes have scant cytoplasm (Figure 7, G and H). The findings of increased osteocyte density, aberrant E11 expression, and absence of a lacuno-canalicular network are all consistent with the presence of woven bone, normally associated with pathologic states of rapid ossification (43).

Consistent with the model that overly rapid maturation of osteoblast maturation results in formation of woven bone, expression of bone sialoprotein (*BSP*), a gene expressed at high levels in woven bone (44), was upregulated almost 20-fold in differentiating $G_s\alpha$-deficient calvarial osteoblasts as compared with control osteoblasts in vitro (Figure 7I). Thus, in the absence of $G_s\alpha$, osteoblast differentiation was accelerated and resulted in production of mainly woven bone, with a failure of production of normal lamellar bone. We suggest that the presence of predominantly woven bone (Figure 2P and Figure 3H) contributes to the remarkable fragility of $G_s\alpha^{OsxKO}$ bones.

Inhibition of canonical Wnt signaling is associated with reduced mesenchymal commitment to the osteoblast lineage in $G_s\alpha^{OsxKO}$ mice. Despite the profound osteoporosis and the scarcity of osteoblasts seen in $G_s\alpha^{OsxKO}$ mice, we have paradoxically found that osteoblast differentiation is dramatically enhanced by the absence of $G_s\alpha$. Since there was no detectable difference in apoptosis by TUNEL staining (Supplemental Figure 3, B and C), and no defect in proliferation of $G_s\alpha$-deficient osteoblasts (Figure 6F and Supplemental Figure 3A), accelerated differentiation into osteocytes should have led to the depletion of the osteoblast population. However, osteoblast numbers were so dramatically reduced (by >80%) in mutant mice (Figure 2K) that we hypothesized that there might also be a decrease in the population of osteoblast precursors. To determine whether osteoblast precursors are reduced in $G_s\alpha^{OsxKO}$ mice, we plated BMSCs and calvarial cells isolated from $G_s\alpha^{OsxKO}$ and control mice at low density, and counted cells capable of initiating fibroblastic colonies (CFU-F) as well as cells capable of initiating osteogenic colonies (CFU-ALP). We found that both CFU-F and CFU-ALP were reduced by greater than 3-fold in $Gs\alpha^{OsxKO}$ BMSCs (Figure 8A). In calvarial cells, while the number of CFU-F was not significantly decreased, the number of CFU-ALP was also markedly lower in $G_s\alpha^{OsxKO}$ mice (Figure 8B).

Canonical Wnt signaling positively regulates osteoblast commitment and differentiation (18–20). Several groups have demonstrated that sclerostin and Dkk1, two inhibitors of Wnt signaling, are potently suppressed by PTH (22, 23, 25). Since $G_s\alpha$ mediates the activation of PKA by PTH stimulation of the PPR, we hypothesized that sclerostin and/or Dkk1 expression would be increased in the absence of $G_s\alpha$. Indeed, *Sost* mRNA, which encodes sclerostin, was markedly increased in calvariae and long bones of $G_s\alpha^{OsxKO}$ mice (Figure 8C and data not shown). Immunohistochemical staining of cortical bone of tibiae at 3 weeks demonstrated abundant sclerostin protein in $G_s\alpha^{OsxKO}$ osteocytes (Figure 8, D and E). Since the increased *Sost* mRNA levels in $G_s\alpha^{OsxKO}$ bones might have at least partially reflected the increase in osteocyte density, we examined expression of *Sost* as well as *Dkk1* mRNAs in cultured calvarial osteoblasts plated at equal numbers. In differentiating calvarial osteoblasts, mRNA levels of both *Sost* and *Dkk1* were dramatically upregulated in $G_s\alpha$-deficient osteoblasts after only 6 days in culture (Figure 8F). Therefore, absence of $G_s\alpha$ in the osteoblast lineage is associated with increased expression of at least two inhibitors of canonical Wnt signaling.

To examine the consequences of upregulation of sclerostin and Dkk1 on Wnt signaling in osteoblasts lacking $G_s\alpha$, we quantitated the expression of the Wnt target genes *Axin2* and *Lef1*. Expression of *Axin2* and *Lef1* mRNAs was significantly reduced in $G_s\alpha$-deficient osteoblasts (Figure 8G). To further evaluate Wnt-dependent signaling in $G_s\alpha$-deficient osteoblasts in vivo, we crossed $G_s\alpha^{OsxKO}$ mice to TopGal reporter mice, in which multiple TCF response elements regulate expression of β-gal (45). Quantitative real-time PCR analysis of mRNA from $G_s\alpha^{OsxKO}$ bones revealed decreased expression of the Wnt reporter TopGal in the absence of $G_s\alpha$ (Figure 8H). Thus, absence of $G_s\alpha$ in the osteoblast lineage leads to increased expression of sclerostin and Dkk1, which may feed back to decrease canonical Wnt signaling in the osteoblast lineage. Since canonical Wnt signaling is required for commitment of mesenchymal progenitors into the osteoblast lineage, attenuated Wnt signaling likely contributes to the reduction of committed osteoprogenitors in $G_s\alpha^{OsxKO}$ mice.

Discussion

The role of $G_s\alpha$ in governing osteoblast differentiation is of particular relevance for several human skeletal disorders (46). Heterozygous loss-of-function mutations in $G_s\alpha$ result in Albright hereditary osteodystrophy (AHO), with short stature, brachydactyly, and obesity. A subset of patients with AHO, frequently those with paternal inheritance of the mutated allele, experience ectopic ossifications that can involve subcutaneous or deep soft tissues as well as skeletal muscle (progressive osseous heteroplasia). Conversely, activating somatic mutations of $G_s\alpha$ are found in fibrous dysplasia, skeletal lesions that can occur alone or in association with other endocrinopathies (McCune-Albright syndrome). Fibrous dysplasia lesions are characterized by impaired osteoblast differentiation and woven bone. Therefore $G_s\alpha$ plays a crucial role in osteoblast development and function, and understanding the molecular mechanisms will be of great clinical significance.

To that end we have generated mice with conditional deletion of $G_s\alpha$ early in the osteoblast lineage. $G_s\alpha^{OsxKO}$ mice have severe osteoporosis characterized by impaired endochondral and intramembranous ossification. The dramatic reduction in bone mass is accompanied by a failure of normal bone formation, with production of predominantly woven bone of inadequate mass and strength, and a marked decrease in osteoblast number. $G_s\alpha$ is downstream of multiple GPCRs and therefore may participate in various signaling pathways. We have identified at least two distinct mechanisms that may underlie the diminished osteoblast number in $G_s\alpha^{OsxKO}$ mice: (a) accelerated differentiation of osteoblasts into osteocytes and (b) decreased commitment of mesenchymal progenitors to the osteoblast lineage, in association with attenuated Wnt signaling that results at least in part from increased expression of the Wnt inhibitors sclerostin and Dkk1.

We have found that the population of osteoblast precursors (CFU-ALP) was significantly decreased among both BMSCs and calvarial cells of $G_s\alpha^{OsxKO}$ mice, suggesting reduced commitment of mesenchymal progenitors to the osteoblast lineage. Wnt signaling is required for osteoblast commitment and early osteoblast differentiation (18–20), and PKA signaling downstream of the PPR can suppress expression of the canonical Wnt inhibitors sclerostin and Dkk1. Sclerostin was overexpressed in calvariae of $G_s\alpha^{OsxKO}$ mice, and both *Sost* and *Dkk1* mRNA levels were increased in cal-

varial osteoblasts from $G_s\alpha^{OsxKO}$ mice, with a concomitant decrease in expression of Wnt target genes in these same cells. Therefore, the inhibition of Wnt signaling may contribute to the dramatic decrease in the pool of osteoprogenitors in $G_s\alpha^{OsxKO}$ mice. In addition to sclerostin and Dkk1, several laboratories have demonstrated other points of interaction between the PTH/PPR/PKA and Wnt signaling pathways (21, 47). PTH is able to activate β-catenin targets in osteoblasts even in the absence of Dkk1 suppression (25, 26), implicating other actions downstream of the PPR in regulating Wnt signaling. Indeed, several potential mechanisms have been identified, including direct interactions between PPR and the Wnt coreceptor LRP6 (48), as well as phosphorylation of β-catenin by PKA (49). Therefore, the effects of PKA on Wnt signaling may be both indirect, mediated by soluble inhibitors such as sclerostin and Dkk1, as well as cell autonomous, by direct phosphorylation of components of the Wnt signaling pathway. More detailed investigations into the effects of $G_s\alpha$ ablation on Wnt signaling in $G_s\alpha^{OsxKO}$ mice are underway.

Once mesenchymal progenitors are committed to the osteoblast lineage, however, the loss of $G_s\alpha$ somewhat paradoxically results in accelerated osteogenic maturation. Although the near absence of osteocalcin mRNA initially suggested a failure of osteoblast differentiation, instead the reduced expression of osteocalcin mRNA reflected attenuated PKA signaling in osteoblasts lacking $G_s\alpha$. In support of this, expression of *Mmp13* mRNA, another PKA target gene, was also reduced in $G_s\alpha^{OsxKO}$ bones, while other markers of osteogenic differentiation were still expressed.

Although the number of mature osteoblasts was markedly reduced in $G_s\alpha^{OsxKO}$ mice, this was not due to complete failure of osteoblast differentiation, as these mice have abundant osteocytes, which are derived from terminally differentiated osteoblasts (40). Rather, we have shown that in the absence of $G_s\alpha$, cells of the osteoblast lineage differentiate rapidly into osteocytes. Whereas PTH has been demonstrated to decrease apoptosis in osteoblasts in adult mice (50), we could find no discernible alteration in osteoblast apoptosis in early postnatal $G_s\alpha^{OsxKO}$ mice in vivo. The effects of PTH on osteoblast apoptosis vary greatly by anatomic location (51) as well as means of administration (10). During early postnatal growth, a time of rapid bone formation, perhaps changes in apoptosis may have lesser effects on cell numbers. In addition, there was no evidence of increased proliferation of $G_s\alpha$-deficient osteoblasts in vivo. Thus, accelerated differentiation results in depletion of osteoblasts and accumulation of osteocytes in $G_s\alpha^{OsxKO}$ mice. It therefore appears that in cells of the osteoblast lineage, $G_s\alpha$ restrains cellular differentiation. Of note, the bone that is present in $G_s\alpha^{OsxKO}$ mice is mainly woven bone. By regulating the pace of osteoblast differentiation, $G_s\alpha$ may function to promote the formation of a larger number of osteoblasts and production of more orderly lamellar bone. In the absence of $G_s\alpha$, the resulting bone is largely woven, typically associated with embryonic development and states of pathologically rapid bone formation such as fracture repair.

Our data are in keeping with the findings that continuous exposure of osteoblasts to PTH inhibits differentiation (11, 12). Moreover, in chondrocytes, ablation of either PPR or $G_s\alpha$ leads to accelerated chondrocyte differentiation and hypertrophy, with adverse consequences for skeletal development (13–17). Whether similar mechanisms underlie the effects of $G_s\alpha$ and PKA in inhibiting differentiation of both osteoblasts and chondrocytes is under investigation.

The mechanisms mediating the effects of $G_s\alpha$ on osteoblast lineage commitment and differentiation are distinct and involve both Wnt-dependent and Wnt-independent effects. In particular, like Wnt signaling and perhaps through its effects on Wnt signaling, $G_s\alpha$ favors osteogenic commitment of mesenchymal progenitors. In contrast, whereas Wnt signaling positively regulates osteoblast differentiation, osteoblast maturation is accelerated in $G_s\alpha^{OsxKO}$ mice even in the face of reduced Wnt signaling, suggesting that absence of $G_s\alpha$ can override the inhibition of Wnt signaling in driving osteoblast differentiation forward. The accelerated differentiation of osteoblasts into osteocytes in the absence of $G_s\alpha$ is unlikely to be related to alterations in Wnt signaling. In differentiated osteoblasts, manipulation of Wnt signaling does not affect bone formation, but only affects bone resorption via disruption of osteoprotegerin expression (52, 53). Furthermore, reduced Wnt signaling in osteocytes due to either ablation of β-catenin or overexpression of Dkk1 in osteoblasts does not lead to an increase in osteocyte density or woven bone (25, 27, 54). Together these studies suggest that Wnt signaling probably does not regulate differentiation of osteoblasts into osteocytes.

The actions of $G_s\alpha$ on both commitment to and differentiation of the osteoblast lineage are at work in both intramembranous and endochondral bone. When plated at low cell densities, osteoprogenitor numbers, as determined by CFU-ALP, were reduced in both BMSCs and calvarial cells of $G_s\alpha^{OsxKO}$ mice. In cells committed to the osteoblast lineage, however, the absence of $G_s\alpha$ resulted in accelerated osteoblast differentiation. In keeping with a similar role for $G_s\alpha$ in both types of cells, when equal numbers of osteoprogenitors were plated in vitro, followed by ablation of $G_s\alpha$, mineralization was dramatically increased in both BMSCs and calvarial cells. Therefore, we conclude that $G_s\alpha$ acts to enhance osteoblast lineage commitment but restrain osteoblast differentiation in both intramembranous and endochondral bone.

The relevant receptors upstream of $G_s\alpha$ are of great interest. The PPR is a prime candidate, since PTH has important effects on osteoblasts, and many of these are mediated by $G_s\alpha$ (10). In vitro, deletion of the PPR in calvarial osteoblasts also resulted in accelerated osteogenic differentiation; however, ablation of the PPR in osteoprogenitors did not lead to the presence of fractures at birth (data not shown). Therefore, other GPCRs may well be involved. Other $G_s\alpha$-coupled GPCRs reported in osteoblasts include TSHR and β2AR. However, ablation of TSHR leads to a high-turnover osteoporosis (31), while deletion of β2AR results in high bone mass (32). Thus, the actions of these receptors are unlikely, at least during embryonic development, to be the predominant GPCRs signaling to $G_s\alpha$ in early cells of the osteoblast lineage. PGE_2 also has anabolic effects on bone (55, 56), and in osteoblasts the PGE_2 receptors EP2 and EP4 are coupled to $G_s\alpha$ and may serve crucial functions in regulating bone formation.

In summary, our studies demonstrate that $G_s\alpha$ signaling early in the osteoblast lineage is crucial for the formation of normal bone. In the absence of $G_s\alpha$, decreased commitment of mesenchymal progenitors to the osteoblast lineage and pathologically accelerated osteogenic differentiation yield bone of striking fragility. That $G_s\alpha$ mediates multiple functions in osteoblasts suggests that more specific targeted interventions may be possible to increase bone mass, quality, and strength.

Methods

Experimental animals. Osx1-GFP::Cre (20) and $G_s\alpha^{fl/fl}$ (57) mice have been described previously. Col2.3::GFP mice (38) were provided by David Rowe (University of Connecticut Health Center, Farmington, Connecticut, USA).

R26 reporter mice were obtained from The Jackson Laboratory. Since $G_s\alpha^{OsxKO}$ mice are of a mixed genetic background (C57BL/6 and CD1), littermate controls ($G_s\alpha^{fl/fl}$, except where otherwise specified) were used for all experiments described. Genotyping was performed on genomic DNA isolated from tails, using previously published protocols (34). All animals were housed in the Center for Comparative Medicine at the Massachusetts General Hospital, and all experiments were approved by the hospital's Subcommittee on Research Animal Care.

Skeletal preparations. Skeletons were fixed in 95% ethanol, then stained overnight in 0.015% alcian blue in acetic acid/ethanol. Soft tissues were cleared in 1% KOH, then stained overnight in 0.01% alizarin red.

Serum TRACP 5b and osteocalcin. Serum levels of TRACP 5b were measured by ELISA using the MouseTRAP assay (Immunodiagnostic Systems). Serum osteocalcin levels were determined by ELISA (Biomedical Technologies Inc.) according to the manufacturer's protocol.

Histological analysis. Mouse limbs were fixed in 10% buffered formalin, paraffin embedded, and sectioned. In situ hybridization was performed according to published protocols (4). Immunohistochemical analysis was performed on deparaffinized sections using biotinylated mouse anti-Sost antibody (R&D Systems) and anti-E11 (eBioscience). Bodian staining to highlight the osteocytic lacuno-canalicular network was performed as described previously (58). For transmission electron microscopy, limbs were fixed in EM fixative (2.5% glutaraldehyde, 2.0% PFA, 0.025% calcium chloride in a 0.1 M sodium cacodylate buffer [pH 7.4]) and processed for EM. Samples were examined with a Phillips 301 transmission electron microscope, and digital images were captured using an Advanced Microscopy Techniques CCD camera.

Histomorphometry and micro-CT analysis. Double calcein labeling was performed by injection of mice with 20 mg/kg calcein on P3 and P6. Mice were sacrificed on P7, and bones were fixed in 10% buffered formalin and embedded in methylmethacrylate as previously described (59). Histomorphometry was carried out in the lower primary spongiosa of the proximal tibia, starting 150 μm below the growth plate and extending for 750 μm, according to standard procedures. Osteocyte density per bone area was quantitated on high-power fields of cortical bone using OsteoMeasure software (OsteoMetrics). For micro-CT analysis, mid-diaphysis areas of femurs were scanned to evaluate cortical bone microarchitecture using a desktop high-resolution micro-CT instrument (μCT40, SCANCO Medical), as described previously (60). In brief, a total of 30 slices for the cortical region were measured at the mid-diaphysis of each femur using an X-ray energy of 70 KeV, integration time of 200 ms, and a 12-μm isotropic voxel size. Cortical shells were contoured across the 30 slices excluding the bone marrow cavity, and the ratio of cortical bone area to the total cross-sectional area was calculated.

Cell culture. Calvarial osteoblasts were harvested from $G_s\alpha^{OsxKO}$ and control mice by serial collagenase digestion as previously described (61), plated at 5×10^3 to 10×10^3 cells/cm^2, and induced to undergo osteogenic differentiation in the presence of ascorbic acid (50 μg/ml) and β-glycerol phosphate (10 mM). $G_s\alpha^{fl/fl}$ calvarial osteoblasts were harvested and subjected to adenoviral infection with adeno-Cre or adeno–β-gal, then induced to undergo osteogenic differentiation as above. For measurement of cAMP accumulation, cells grown in 24-well plates were incubated at 37°C for 15 minutes in a buffer containing 2 mM isobutyl methylxanthine (an inhibitor of phosphodiesterase activity). Intracellular levels of cAMP were determined by radioimmunoassay as previously described (62).

BMSCs were harvested from neonatal mice by crushing hind limbs in PBS containing 2% fetal bovine serum. Bone marrow cells were filtered and plated at 0.5×10^6 to 1×10^6 cells/cm^2 and subjected to osteogenic differentiation as described above.

CFU assays. BMSCs and calvarial cells from WT and KO mice were seeded at 50×10^3 cells/cm^2 and 100 cells/cm^2, respectively, on Primaria cell culture plates (BD Falcon). For CFU-F assays, colonies were cultured for 7 days in α-MEM plus 10% fetal bovine serum, then fixed with formalin and stained with methylene blue. For CFU-ALP assays, colonies were cultured in osteogenic media containing 10 mM β-glycerol phosphate and 50 μg/ml ascorbic acid (both from Sigma-Aldrich). After 7 days colonies were fixed in formalin and stained for ALP activity as described previously (63).

Flow cytometry. Osteoblastic cells were harvested from neonatal calvariae of Col2.3::GFP;$G_s\alpha^{fl/fl}$ mice by serial collagenase digestion (61). Fractions 3–6 were pooled and resuspended in PBS with 2% fetal bovine serum. Cells were stained with biotinylated anti-ALP antibody (64) (courtesy of Mark Horowitz, Yale University, New Haven, Connecticut, USA) and streptavidin-APC (eBioscience), then analyzed on a FACSCalibur flow cytometer (BD Biosciences).

Quantitative real-time PCR. Total RNA was isolated using the RNeasy kit (QIAGEN), and cDNA was synthesized with the SuperScript III First Strand synthesis system for real-time PCR (Invitrogen). Quantitative real-time PCR was performed using primers for $G_s\alpha$ (13), Runx2 (65), ALP (65), Osx (65), Col1a1 (66), Atf4 (66), Sost (67), TopGal (25), Dmp1 (67), Phex (67), and BSP (65) according to previously published protocols, with mRNA levels normalized to β-actin expression. Total RNA samples subjected to cDNA synthesis reactions in the absence of reverse transcriptase were included as negative controls.

Statistics. Statistical analyses were performed using a 2-tailed Student's *t* test. All values are expressed as mean ± SEM. *P* values less than 0.05 were considered significant.

Acknowledgments

We thank David Rowe for providing the Col2.3::GFP transgenic mice; Mark Horowitz for providing the ALP antibody; James Oh, Jackie McConnell, and Rhiannon Chubb for technical assistance; the MGH Center for Comparative Medicine staff for care of the mice; and the Dana Farber Cancer Institute and Harvard Stem Cell Institute flow cytometry cores. This work was supported in part by NIH grants AR053781 (to J.Y. Wu) and DK117940 (to H.M. Kronenberg) and by the National Institute of Diabetes and Digestive and Kidney Diseases' Intramural Research Program (to M. Chen and L.S. Weinstein).

Received for publication January 13, 2011, and accepted in revised form June 8, 2011.

Address correspondence to: Joy Y. Wu or Henry M. Kronenberg, Endocrine Unit, Massachusetts General Hospital, 50 Blossom Street, Thier 1101, Boston, Massachusetts 02114, USA. Phone: 617.726.3966; Fax: 617.726.7543; E-mail: jywu@partners.org (J.Y. Wu), hkronenberg@partners.org (H.M. Kronenberg).

1. Raisz LG. Pathogenesis of osteoporosis: concepts, conflicts, and prospects. *J Clin Invest*. 2005; 115(12):3318–3325.
2. Neer RM, et al. Effect of parathyroid hormone (1-34) on fractures and bone mineral density in postmenopausal women with osteoporosis. *N Engl J Med*. 2001;344(19):1434–1441.
3. Bringhurst FR, et al. Cloned, stably expressed parathyroid hormone (PTH)/PTH-related peptide receptors activate multiple messenger signals and biological responses in LLC-PK1 kidney cells. *Endocrinology*. 1993;132(5):2090–2098.
4. Calvi LM, et al. Activated parathyroid hormone/parathyroid hormone-related protein receptor in osteoblastic cells differentially affects cortical and trabecular bone. *J Clin Invest*. 2001;107(3):277–286.
5. Schipani E, Kruse K, Juppner H. A constitutively active mutant PTH-PTHrP receptor in Jansen-type metaphyseal chondrodysplasia. *Science*. 1995; 268(5207):98–100.
6. Pearman AT, Chou WY, Bergman KD, Pulumati MR, Partridge NC. Parathyroid hormone induces c-fos promoter activity in osteoblastic cells through phosphorylated cAMP response element (CRE)-binding protein binding to the major CRE. *J Biol Chem*. 1996;271(41):25715–25721.
7. Weinstein LS, Yu S, Warner DR, Liu J. Endocrine

manifestations of stimulatory G protein alpha-subunit mutations and the role of genomic imprinting. *Endocr Rev*. 2001;22(5):675–705.
8. Bianco P, Kuznetsov SA, Riminucci M, Fisher LW, Spiegel AM, Robey PG. Reproduction of human fibrous dysplasia of bone in immunocompromised mice by transplanted mosaics of normal and Gsalpha-mutated skeletal progenitor cells. *J Clin Invest*. 1998;101(8):1737–1744.
9. Hsiao EC, et al. Osteoblast expression of an engineered Gs-coupled receptor dramatically increases bone mass. *Proc Natl Acad Sci U S A*. 2008; 105(4):1209–1214.
10. Jilka RL. Molecular and cellular mechanisms of the anabolic effect of intermittent PTH. *Bone*. 2007; 40(6):1434–1446.
11. Ishizuya T, et al. Parathyroid hormone exerts disparate effects on osteoblast differentiation depending on exposure time in rat osteoblastic cells. *J Clin Invest*. 1997;99(12):2961–2970.
12. Wang YH, Liu Y, Buhl K, Rowe DW. Comparison of the action of transient and continuous PTH on primary osteoblast cultures expressing differentiation stage-specific GFP. *J Bone Miner Res*. 2005;20(1):5–14.
13. Bastepe M, et al. Stimulatory G protein directly regulates hypertrophic differentiation of growth plate cartilage in vivo. *Proc Natl Acad Sci U S A*. 2004;101(41):14794–14799.
14. Chung UI, Lanske B, Lee K, Li E, Kronenberg H. The parathyroid hormone/parathyroid hormone-related peptide receptor coordinates endochondral bone development by directly controlling chondrocyte differentiation. *Proc Natl Acad Sci U S A*. 1998; 95(22):13030–13035.
15. Kozhemyakina E, Cohen T, Yao TP, Lassar AB. Parathyroid hormone-related peptide represses chondrocyte hypertrophy through a protein phosphatase 2A/histone deacetylase 4/MEF2 pathway. *Mol Cell Biol*. 2009;29(21):5751–5762.
16. Lanske B, et al. PTH/PTHrP receptor in early development and Indian hedgehog-regulated bone growth. *Science*. 1996;273(5275):663–666.
17. Sakamoto A, Chen M, Kobayashi T, Kronenberg HM, Weinstein LS. Chondrocyte-specific knockout of the G protein G(s)alpha leads to epiphyseal and growth plate abnormalities and ectopic chondrocyte formation. *J Bone Miner Res*. 2005;20(4):663–671.
18. Day TF, Guo X, Garrett-Beal L, Yang Y. Wnt/beta-catenin signaling in mesenchymal progenitors controls osteoblast and chondrocyte differentiation during vertebrate skeletogenesis. *Dev Cell*. 2005;8(5):739–750.
19. Hill TP, Spater D, Taketo MM, Birchmeier W, Hartmann C. Canonical Wnt/beta-catenin signaling prevents osteoblasts from differentiating into chondrocytes. *Dev Cell*. 2005;8(5):727–738.
20. Rodda SJ, McMahon AP. Distinct roles for Hedgehog and canonical Wnt signaling in specification, differentiation and maintenance of osteoblast progenitors. *Development*. 2006;133(16):3231–3244.
21. Kulkarni NH, et al. Effects of parathyroid hormone on Wnt signaling pathway in bone. *J Cell Biochem*. 2005;95(6):1178–1190.
22. Bellido T, et al. Chronic elevation of parathyroid hormone in mice reduces expression of sclerostin by osteocytes: a novel mechanism for hormonal control of osteoblastogenesis. *Endocrinology*. 2005; 146(11):4577–4583.
23. Keller H, Kneissel M. SOST is a target gene for PTH in bone. *Bone*. 2005;37(2):148–158.
24. Leupin O, et al. Control of the SOST bone enhancer by PTH using MEF2 transcription factors. *J Bone Miner Res*. 2007;22(12):1957–1967.
25. Guo J, et al. Suppression of Wnt signaling by Dkk1 attenuates PTH-mediated stromal cell response and new bone formation. *Cell Metabolism*. 2010; 11(2):161–171.
26. Yao GQ, Wu JJ, Troiano N, Insogna K. Targeted overexpression of Dkk1 in osteoblasts reduces bone mass but does not impair the anabolic response to intermittent PTH treatment in mice. *J Bone Miner Metab*. 2011;29(2):141–148.
27. Li J, et al. Dkk1-mediated inhibition of Wnt signaling in bone results in osteopenia. *Bone*. 2006; 39(4):754–766.
28. Winkler DG, et al. Osteocyte control of bone formation via sclerostin, a novel BMP antagonist. *EMBO J*. 2003;22(23):6267–6276.
29. O'Brien CA, et al. Control of bone mass and remodeling by PTH receptor signaling in osteocytes. *PLoS One*. 2008;3(8):e2942.
30. Suda M, et al. Prostaglandin E receptor subtypes in mouse osteoblastic cell line. *Endocrinology*. 1996; 137(5):1698–1705.
31. Abe E, et al. TSH is a negative regulator of skeletal remodeling. *Cell*. 2003;115(2):151–162.
32. Elefteriou F, et al. Leptin regulation of bone resorption by the sympathetic nervous system and CART. *Nature*. 2005;434(7032):514–520.
33. Sakamoto A, Chen M, Nakamura T, Xie T, Karsenty G, Weinstein LS. Deficiency of the G-protein alpha-subunit G(s)alpha in osteoblasts leads to differential effects on trabecular and cortical bone. *J Biol Chem*. 2005;280(22):21369–21375.
34. Wu J, et al. Osteoblastic regulation of B lymphopoiesis is mediated by Gsalpha-dependent signaling pathways. *Proc Natl Acad Sci U S A*. 2008; 105(44):16976–16981.
35. Boguslawski G, et al. Activation of osteocalcin transcription involves interaction of protein kinase A and protein kinase C-dependent pathways. *J Biol Chem*. 2000;275(2):999–1006.
36. Selvamurugan N, Chou WY, Pearman AT, Pulumati MR, Partridge NC. Parathyroid hormone regulates the rat collagenase-3 promoter in osteoblastic cells through the cooperative interaction of the activator protein-1 site and the runt domain binding sequence. *J Biol Chem*. 1998;273(17):10647–10657.
37. Soriano P. Generalized lacZ expression with the ROSA26 Cre reporter strain. *Nat Genet*. 1999; 21(1):70–71.
38. Kalajzic I, et al. Use of type I collagen green fluorescent protein transgenes to identify subpopulations of cells at different stages of the osteoblast lineage. *J Bone Miner Res*. 2002;17(1):15–25.
39. Bonewald LF, Johnson ML. Osteocytes, mechanosensing and Wnt signaling. *Bone*. 2008;42(4):606–615.
40. Manolagas SC. Birth and death of bone cells: basic regulatory mechanisms and implications for the pathogenesis and treatment of osteoporosis. *Endocr Rev*. 2000;21(2):115–137.
41. Dallas SL, et al. Time lapse imaging techniques for comparison of mineralization dynamics in primary murine osteoblasts and the late osteoblast/early osteocyte-like cell line MLO-A5. *Cells Tissues Organs*. 2009;189(1–4):6–11.
42. Zhang K, et al. E11/gp38 selective expression in osteocytes: regulation by mechanical strain and role in dendrite elongation. *Mol Cell Biol*. 2006; 26(12):4539–4552.
43. Hadjiargyrou M, Rightmire EP, Ando T, Lombardo FT. The E11 osteoblastic lineage marker is differentially expressed during fracture healing. *Bone*. 2001; 29(2):149–154.
44. Gorski JP. Is all bone the same? Distinctive distributions and properties of non-collagenous matrix proteins in lamellar vs. woven bone imply the existence of different underlying osteogenic mechanisms. *Crit Rev Oral Biol Med*. 1998;9(2):201–223.
45. DasGupta R, Fuchs E. Multiple roles for activated LEF/TCF transcription complexes during hair follicle development and differentiation. *Development*. 1999;126(20):4557–4568.
46. Weinstein LS, Chen M, Xie T, Liu J. Genetic diseases associated with heterotrimeric G proteins. *Trends Pharmacol Sci*. 2006;27(5):260–266.
47. Tobimatsu T, et al. Parathyroid hormone increases beta-catenin levels through Smad3 in mouse osteoblastic cells. *Endocrinology*. 2006;147(5):2583–2590.
48. Wan M, et al. Parathyroid hormone signaling through low-density lipoprotein-related protein 6. *Genes Dev*. 2008;22(21):2968–2979.
49. Taurin S, Sandbo N, Qin Y, Browning D, Dulin NO. Phosphorylation of beta-catenin by cyclic AMP-dependent protein kinase. *J Biol Chem*. 2006; 281(15):9971–9976.
50. Jilka RL, Weinstein RS, Bellido T, Roberson P, Parfitt AM, Manolagas SC. Increased bone formation by prevention of osteoblast apoptosis with parathyroid hormone. *J Clin Invest*. 1999;104(4):439–446.
51. Jilka RL, O'Brien CA, Ali AA, Roberson PK, Weinstein RS, Manolagas SC. Intermittent PTH stimulates periosteal bone formation by actions on post-mitotic preosteoblasts. *Bone*. 2009;44(2):275–286.
52. Glass DA 2nd, et al. Canonical Wnt signaling in differentiated osteoblasts controls osteoclast differentiation. *Dev Cell*. 2005;8(5):751–764.
53. Holmen SL, et al. Essential role of beta-catenin in postnatal bone acquisition. *J Biol Chem*. 2005; 280(22):21162–21168.
54. Kramer I, et al. Osteocyte Wnt/beta-catenin signaling is required for normal bone homeostasis. *Mol Cell Biol*. 2010;30(12):3071–3085.
55. Yoshida K, et al. Stimulation of bone formation and prevention of bone loss by prostaglandin E EP4 receptor activation. *Proc Natl Acad Sci U S A*. 2002;99(7):4580–4585.
56. Zhang X, Schwarz EM, Young DA, Puzas JE, Rosier RN, O'Keefe RJ. Cyclooxygenase-2 regulates mesenchymal cell differentiation into the osteoblast lineage and is critically involved in bone repair. *J Clin Invest*. 2002;109(11):1405–1415.
57. Chen M, et al. Increased glucose tolerance and reduced adiposity in the absence of fasting hypoglycemia in mice with liver-specific Gs alpha deficiency. *J Clin Invest*. 2005;115(11):3217–3227.
58. Inoue K, et al. A crucial role for matrix metalloproteinase 2 in osteocytic canalicular formation and bone metabolism. *J Biol Chem*. 2006;281(44):33814–33824.
59. Sims NA, Brennan K, Spaliviero J, Handelsman DJ, Seibel MJ. Perinatal testosterone surge is required for normal adult bone size but not for normal bone remodeling. *Am J Physiol Endocrinol Metab*. 2006;290(3):E456–E462.
60. Bouxsein ML, Boyd SK, Christiansen BA, Guldberg RE, Jepsen KJ, Muller R. Guidelines for assessment of bone microstructure in rodents using micro-computed tomography. *J Bone Miner Res*. 2010; 25(7):1468–1486.
61. Yang D, Guo J, Divieti P, Shioda T, Bringhurst FR. CBP/p300-interacting protein CITED1 modulates parathyroid hormone regulation of osteoblastic differentiation. *Endocrinology*. 2008;149(4):1728–1735.
62. Aydin C, et al. Extralarge XL(alpha)s (XXL(alpha)s), a variant of stimulatory G protein alpha-subunit (Gs(alpha)), is a distinct, membrane-anchored GNAS product that can mimic Gs(alpha). *Endocrinology*. 2009;150(8):3567–3575.
63. Aubin JE. Osteoprogenitor cell frequency in rat bone marrow stromal populations: role for heterotypic cell-cell interactions in osteoblast differentiation. *J Cell Biochem*. 1999;72(3):396–410.
64. Strasser A. PB76: a novel surface glycoprotein preferentially expressed on mouse pre-B cells and plasma cells detected by the monoclonal antibody G-5-2. *Eur J Immunol*. 1988;18(11):1803–1810.
65. Kenner L, et al. Mice lacking JunB are osteopenic due to cell-autonomous osteoblast and osteoclast defects. *J Cell Biol*. 2004;164(4):613–623.
66. Dobreva G, et al. SATB2 is a multifunctional determinant of craniofacial patterning and osteoblast differentiation. *Cell*. 2006;125(5):971–986.
67. Tatsumi S, et al. Targeted ablation of osteocytes induces osteoporosis with defective mechanotransduction. *Cell Metab*. 2007;5(6):464–475.